International Journal of Applied Information Systems (IJAIS) – ISSN : 2249-0868
Foundation of Computer Science FCS, New York, USA
Volume 12 – No. 11, February 2018 – www.ijais.org

Comparison of Analytical Modeling and Numerical modeling of the role of Reverse Parameter using Differential Geometry in Differential Rate Equations of Tm-doped Tellurite Material

Wedad Albalawi
Princess Nourah bint Abdulrahman University
College of sciences,
PO Box 84428
Riyadh, KSA

Ali Albalawi
Swansea University,
Bay Campus, Swansea
United Kingdom, SA1 8EN

ABSTRACT
This paper analytical and numerical investigates the reverse cross relaxation parameter in differential rate equations of Tm-doped tellurite material using differential geometry principles with different dopant concentrations. The comparison between analytical simulation and numerical simulation indicates that there is difference in calculations in case of neglect the reverse cross relaxation parameters in analytical modeling compared with the simulation which respects reverse cross relaxation parameter in numerical modeling. The difference is calculated for a set of samples with concentration level variations by a factor of 30 (0.36 mol% to 10 mol%). This paper shows also the impact of neglect the reverse cross relaxation parameter on the population of Tm-doped tellurite material. It indicates that the role of reverse crosses relaxation impacts according to pump intensity and energy level and it have a significant effect on the simulation of laser and amplifier devices.

General Terms
Reverse cross relaxation parameter, Cross relaxation, Thulium doped material. Differential rate equations.

Keywords
Thulium-doped material. Differential rate equations. Pump power. Reverse cross relaxation parameter. Cross-relaxation.

1. INTRODUCTION
Thulium (Tm^{3+}) is an excellent candidate for infrared laser applications thanks to its broad emission spectrum at around 1.8 micron, which makes it very appealing for several applications from precise cut and ablation of biological tissues to sensing applications [1-6]. Furthermore, Tm^{3+} has a significant property, which is cross-relaxation parameter ($^3H_4$,$^3H_6$,→$^3F_4$,$^3F_4$) where two ions are promoted in the upper level of laser by every single pumping photon. This parameter significantly improves pumping quantum efficiency and lasing at 1.8 µm. Yet most of laser simulations do not consider, or do not directly measure, the reverse cross-relaxation parameter ($^3F_4$,$^3F_4$,→$^3H_6$,$^3H_4$) that reduces the efficacy of cross-relaxation parameter.

Despite the abundant evidences relating to lifetimes and cross-sections, the parameters associated with ion-ion interactions (i.e., cross-relaxation and the reverse transfer process) [7-12] are more difficult to obtain or cannot be identified in a straightforward manner. It is especially notable that such parameters are typically unavailable as parameters, which undergo validation over a wide range of doping levels, and are thus unsuitable for doping level optimization. Some studies are published by the present authors, including [13],[14], have focused on the numerical investigation of the reverse transfer parameter in several samples of Tm-doped tellurite glass, and compare it with experiment data by accurate measurements and best set-up validated by fitting experimental fluorescence decay curves of both $^3H_4$ and $^3F_4$ levels. In those studies, the authors indicated that it is possible to fit a set of samples with doping level variations by a factor of 30 (0.36-10 mol%), where identical parameters are applied for every sample. In addition to this, it demonstrated that can be obtained the reverse cross-relaxation parameter. Noteworthy, those studies adopted a method that is an alternative approach to the one based on Kushida [15]. It defined a as the ratio between reverse and cross relaxation parameter and calculated it as of 0.03 ($P_{22} = a \times P_{41}$), i.e. a was equal 3% in Ref. [13] .

This paper calculates the reverse cross relaxation parameter by numerical modeling and analytical modeling (mathematics) to validate the results by compare the both simulation. This paper shows the deference in the two cases with and without the reverse cross relaxation parameter. It shows that should take into account the whole set of parameters including the reverse cross relaxation to obtain an accurate results and precise measurements.

2. NUMERICAL MODELING
The energy levels scheme is used with transitions that are shown in Fig. 1[8],[16].

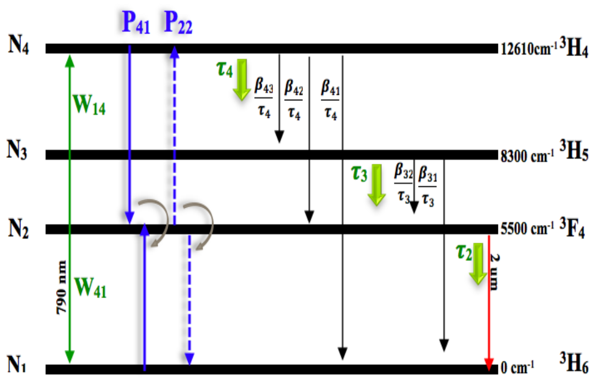

Fig. 1: Lowest four energy levels of Tm-doped glass with the reverse cross relaxation.

Fig.1 shows the lowest four energy manifolds of Tm^{3+} ion. In the figure, the laser transition, the pump transition, and direct and reverse cross-relaxation processes are indicated, together with spontaneous decay paths. The corresponding set of differential rate equations is as follows:

$$\frac{dN_4}{dt} = W_{14}N_1 - W_{41}N_4 - \frac{N_4}{\tau_4} - P_{41}N_4N_1 + P_{22}N_2^2 \quad (1)$$

$$\frac{dN_3}{dt} = -\frac{N_3}{\tau_3} + \frac{\beta_{43}N_4}{\tau_4} \quad (2)$$

$$\frac{dN_2}{dt} = 2P_{41}N_4N_1 - 2P_{22}N_2^2 - \frac{N_2}{\tau_2} + \frac{\beta_{42}N_4}{\tau_4} + \frac{\beta_{32}N_3}{\tau_3} \quad (3)$$

$$\frac{dN_1}{dt} = -W_{14}N_1 + W_{41}N_4 + P_{22}N_2^2 - P_{41}N_4N_1 + \frac{N_2}{\tau_2} + \frac{\beta_{41}N_4}{\tau_4} + \frac{\beta_{31}N_3}{\tau_3} \quad (4)$$

where N_1 ,N_2 ,N_3 and N_4 are the population of the energy levels $^3H_6$ (ground level), $^3F_4$ (upper laser level), $^3H_5$ and $^3H_4$ (pump level), respectively; W_{14} ,W_{41} are the pump rates, τ_i the lifetime of the i-level, and β_{ij} are branch ratios from the *i*- to J-level [12]. The coefficients P_{ij} describe the energy transfer processes: P_{41} ($^3H_4$, $^3H_6 \rightarrow$ $^3F_4$, $^3F_4$) is the cross relaxation constant, which is proportional to doping level [9],[12], and P_{22} ($^3F_4$,$^3F_4$,$\rightarrow$$^3H_6$,$^3H_4$) is the reverse cross-relaxation process constant, the investigation of which is the main aim of this study. This study use the model to calculate and assess the reverse cross relaxation of a set on Tellurite glass samples with doping levels ranging from 0.36 mol% to 10 mol%. Used numerical values are listed in Table 1. The pump cross section at 790 nm was taken from Ref [12] while the emission cross-section was calculated using Ref [17].

Table 1:List of parameters used in the modeling

Parameters	Symb	values		Ref.
Coefficient of Cross Relaxation	Cr	$1.81*10^{-23}$ m^3 s^1 mol^{-1}		[9]
Pump wavelength	λ_p	790 nm		
Cross Relaxation	P_{41}	Mole *Cr (m^3 s^-		[9]
Reverse of Cross relaxation	P_{22}	$0.03*P_{41}$		[13]
Absorption pump cross-section	σ_{ap}	$8*10^{-25}$ m^2		[12]
Emission pump cross-section	σ_{ep}	$2.2*10^{-25}$ m^2		[17] *
Pump Intensity	I_p	$1.3*10^3$ W/cm^2		
Branch ratio	β_{41}	$^3H_4 \rightarrow ^3H_6$	0.903	[12]
	β_{42}	$^3H_4 \rightarrow ^3F_4$	0.076	[12]
	β_{43}	$^3H_4 \rightarrow ^3H_5$	0.02	[12]
	β_{31}	$^3H_5 \rightarrow ^3H_6$	0.979	[12]
	β_{32}	$^3H_5 \rightarrow ^3F_4$	0.020	[12]

*Calculated by McCumber equation from [17]

While many parameters were either easily recalculated as lifetimes or taken by previous publications, as cross-relaxation constant or branching ratios, Authors had to investigate the reverse cross-relaxation process in order to complete the set of parameters and be able to use the set of Eq.1-4 to simulate Tm-doped laser over a wide range of concentrations and evaluate the impact of reverse cross relaxation on the amount of pump power required to a given inversion.

2.1 Numerical Methodology

After defining the differential rate equations (1-4) and the values of the target parameters, the purpose of this section is to discuss the basic methods for the numerical solution of values and the behavior of populations, along with the value of the derivatives. Since the equations used in this paper have taken full parameters within differential geometry, including reverse cross-relaxation (P_{22}), the solutions are expected to be complex. Therefore, it is noteworthy that for most complex differential equations, an analytical solution cannot be obtained, but a numerical solution can almost always be obtained.

Using the MATLAB software, the used rate equations are solved numerically. It is notable that MATLAB contains many functions to solve differential equations, including ordinary differential equation (ODE) solvers and the fsolve function, each of which employs a different numerical method. These functions are usually sufficient for most problems. The first step is to define the function that calculates $\frac{dN_4}{dt}$, $\frac{dN_3}{dt}$, $\frac{dN_2}{dt}$, and $\frac{dN_1}{dt}$ from the concentration of each sample in the steady state condition. In this model, fsolve with a special structure, namely, the "Levenberg-Marquardt algorithm" has been defined to solve the system of nonlinear equations and to find the values of the population numerically. The second step, the initial values are defined separately, and the range for which the differential equations are solved is also defined within the function. The third step, the finite difference algorithm can be executed using the for loop in the following way: (for k = 1:length (p)……… end) where p is pump power. In this way, it can be ensured that the iterations of the calculations will reach the required pump power value (i.e., 1 W), since p is increased by a factor of $1*10^{-4}$. Following this, the algorithm proceeds to the next iteration. The simulation is implemented and the results of concentrations against the pump power values are plotted (as shown in Figures 2 and 3 for the $^3F_4$ and $^3H_4$ populations, respectively).

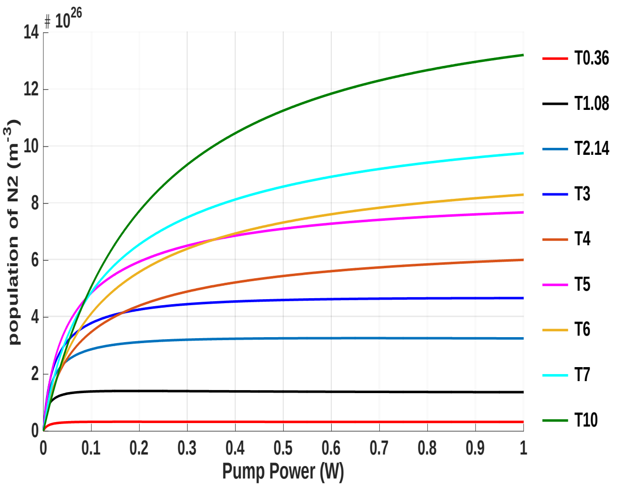

Fig. 2: Numerical simulation of Populations of the $^3F_4$ level vs. the pump power

International Journal of Applied Information Systems (IJAIS) – ISSN : 2249-0868
Foundation of Computer Science FCS, New York, USA
Volume 12 – No. 11, February 2018 – www.ijais.org

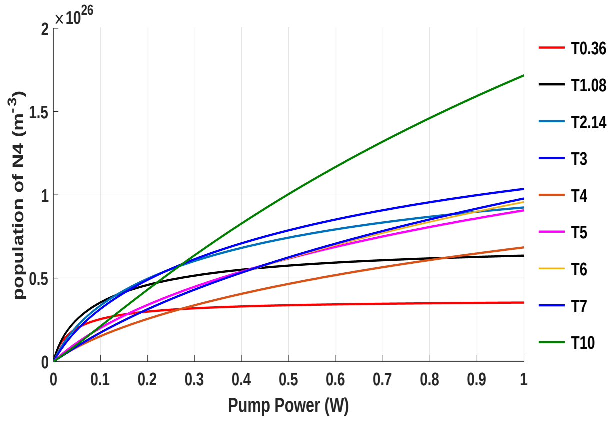

Fig. 3: Numerical simulation of Populations of the $^3H_4$ level vs. the pump power

3. ANALYTICAL MODELING

The analytical part of this paper used the same energy levels scheme and considered the same transitions with neglecting reverse cross-relaxation.

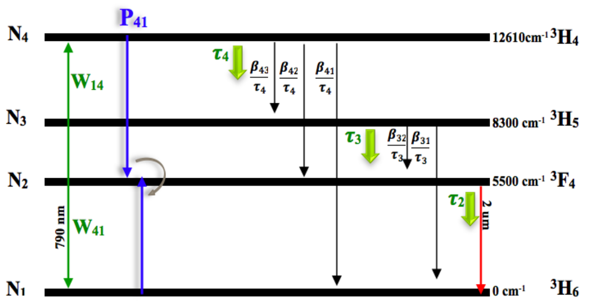

Fig. 4: Lowest four energy levels of Tm-doped glass (reverse cross-relaxation)

Fig. 4 shows the lowest four energy levels of the Tm^{3+} ion. In the figure, the laser transition, the pump transition, and cross-relaxation process are indicated, together with spontaneous decay paths. The corresponding set of differential rate equations without the reverse cross relaxation parameters is follows:

$$\frac{dN_4}{dt} = W_{14}N_1 - W_{41}N_4 - \frac{N_4}{\tau_4} - P_{41}N_4N_1 \quad (5)$$

$$\frac{dN_3}{dt} = -\frac{N_3}{\tau_3} + \frac{\beta_{43}N_4}{\tau_4} \quad (6)$$

$$\frac{dN_2}{dt} = 2P_{41}N_4N_1 - \frac{N_2}{\tau_2} + \frac{\beta_{42}N_4}{\tau_4} + \frac{\beta_{32}N_3}{\tau_3} \quad (7)$$

$$\frac{dN_1}{dt} = -W_{14}N_1 + W_{41}N_4 - P_{41}N_4N_1 + \frac{N_2}{\tau_2} + \frac{\beta_{41}N_4}{\tau_4} + \frac{\beta_{31}N_3}{\tau_3} \quad (8)$$

Through solving the rate equations at steady state analytically, this research calculates the population values for each level (N_1, N_2, N_3, N_4) mathematically without considering the reverse cross-relaxation as follow:

First of all let

$$A_4 = \frac{1}{\tau_4}, A_3 = \frac{1}{\tau_3} \quad A_{42} = \frac{\beta_{42}}{\tau_4}, \quad A_{32} = \frac{\beta_{32}}{\tau_3}, \text{ and } A_{43} = \frac{\beta_{43}}{\tau_4}$$

The values of N_4, N_3 and N_2 are

$$N_4 = \frac{W_{14}N_1}{W_{41}+A_4+P_{41}N_1} \quad (9)$$

$$N_3 = \left(\frac{A_{43}}{A_3}\right)\frac{W_{14}N_1}{W_{41}+A_4+P_{41}N_1} \quad (10)$$

$$N_2 = \left(\frac{2P_{41}N_1}{A_2} * \frac{W_{14}N_1}{W_{41}+A_4+P_{41}N_1}\right) + \left(\frac{A_{42}}{A_2} * \frac{W_{14}N_1}{W_{41}+A_4+P_{41}N_1}\right) + \left(\frac{A_{32}}{A_2} * \frac{\left(\frac{A_{43}}{A_3}\right)W_{14}N_1}{W_{41}+A_4+P_{41}N_1}\right) \quad (11)$$

Using

$$N_{tot} = N_1 + N_2 + N_3 + N_4 \quad (12)$$

By substitute N_2, N_4 and N_3 From Eq. (9), (10) and (11) in Eq. (12)

$$N_{tot} = N_1 + \left(\frac{2P_{41}N_1}{A_2} * \frac{W_{14}N_1}{W_{41}+A_4+P_{41}N_1}\right) + \left(\frac{A_{42}}{A_2} * \frac{W_{14}N_1}{W_{41}+A_4+P_{41}N_1}\right) + \left(\frac{A_{32}}{A_2} * \frac{\left(\frac{A_{43}}{A_3}\right)W_{14}N_1}{W_{41}+A_4+P_{41}N_1}\right) + \frac{\left(\frac{A_{43}}{A_3}\right)W_{14}N_1}{W_{41}+A_4+P_{41}N_1} + \frac{W_{14}N_1}{W_{41}+A_4+P_{41}N_1}$$

To simply, let

$$b = \frac{2P_{41}W_{14}}{A_2}, c = \frac{A_{42}W_{14}}{A_2}, r = \frac{A_{32}hW_{14}}{A_2},$$

$$H = W_{41} + A_4 + P_{41}N_1$$

Thus

$$N_{tot} = N_1 + \left(\frac{bN_1^2}{W_{41}+A_4+P_{41}N_1} + \frac{cN_1}{W_{41}+A_4+P_{41}N_1} + \frac{rN_1}{W_{41}+A_4+P_{41}N_1}\right) + \frac{\left(\frac{A_{43}}{A_3}\right)W_{14}N_1}{W_{41}+A_4+P_{41}N_1} + \frac{W_{14}N_1}{W_{41}+A_4+P_{41}N_1}$$

By let

$$C = N_{tot}W_{41} + N_{tot}A_4$$

$$B = \left(-N_{tot}P_{41} + W_{41} + A_4 + c + r + \left(\frac{A_{43}}{A_3}\right)W_{14} + W_{14}\right)$$

$$A = P_{41} + b$$

Then using the general low to obtain N_1

$$N_1 = \frac{+B - \sqrt{B^2 + 4 * A * C}}{-2A}$$

Then the simulation is implemented and the results of concentrations against the pump power values are plotted analytically (as shown in Figures 5 and 6 for the $^3F_4$ and $^3H_4$ populations, respectively).

International Journal of Applied Information Systems (IJAIS) – ISSN : 2249-0868
Foundation of Computer Science FCS, New York, USA
Volume 12 – No. 11, February 2018 – www.ijais.org

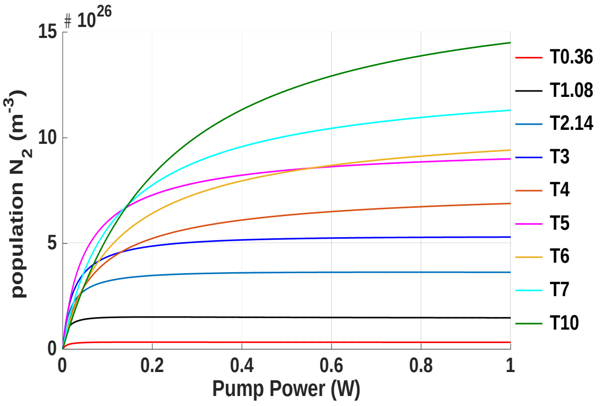

Fig. 5: Analytical simulation of Populations of the $^3F_4$ level vs. the pump power

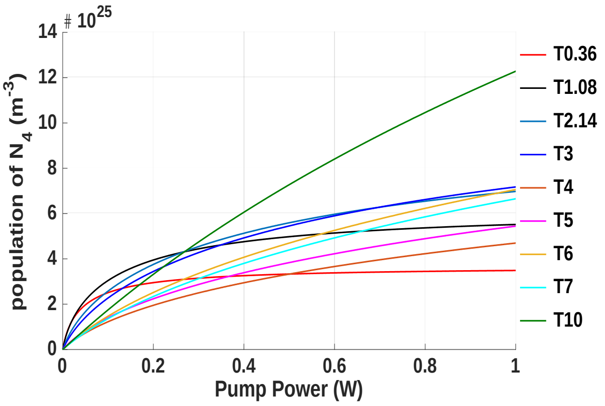

Fig. 6: Analytical simulation of Populations of the $^3H_4$ level vs. the pump power

4. VALIDATING OF SIMULATIONS

This analytical method can be used to validate the numerical technique that was developed in section 2 when there is no reverse cross-relaxation. Therefore, it is compared with numerical simulation with the assumption of the reverse of cross-relaxation equal to zero in numerical simulation. In this case, the result is identical between analytical and numerical simulation, indicating the validity of the approach, for example as shown in Fig. 7 in case of sample T4 for both $^3F_4$.

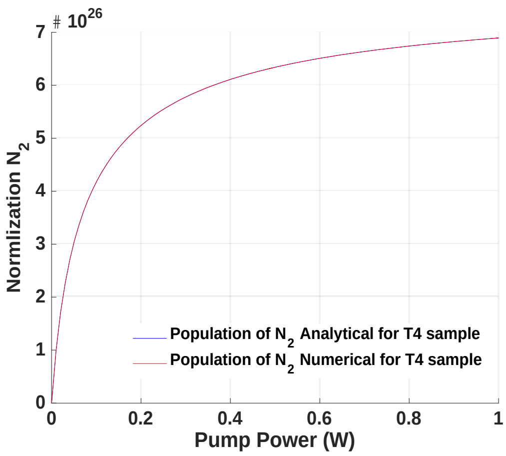

Fig.7: Comparison between analytical simulation (neglecting P_{22}) and numerical simulation (with P_{22}=0) for $^3F_4$ level of sample T4

5. RESULT AND DISCUSSION

The calculations from the mentioned models can assist with the design process and they can also be utilised to examine the population of the thulium-doped tellurite systems. Through solving the differential rate equations, the populations in levels 4, 3, 2, and 1 are calculated for all samples. [18]. The population at each level were compared with same population in numerical simulation which investigated in Ref [13]. It is clear that the difference is obvious and vary according to pump power and energy level as shown in Fig. 4 (a),(b),(c), and (d), which illustrates the populations as a function of pump power of $^3H_6$, $^3F_4$,$^3H_5$, and $^3H_4$ respectively for both analytical simulation with no consider reverse cross relaxation and numerical simulation with reverse cross relaxation. It is noticeable also that as the pump intensity increase as the difference increases.

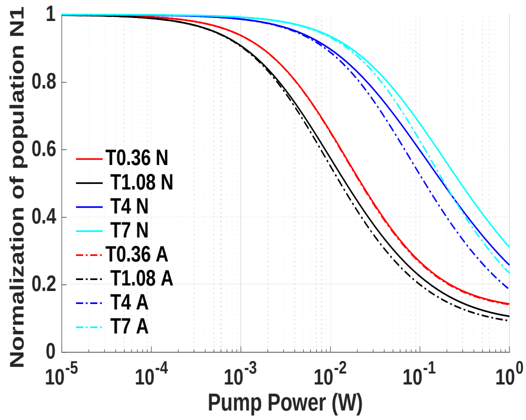

(a)

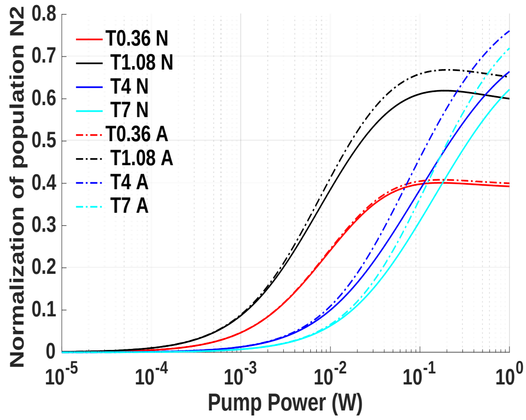

(b)

International Journal of Applied Information Systems (IJAIS) – ISSN : 2249-0868
Foundation of Computer Science FCS, New York, USA
Volume 12 – No. 11, February 2018 – www.ijais.org

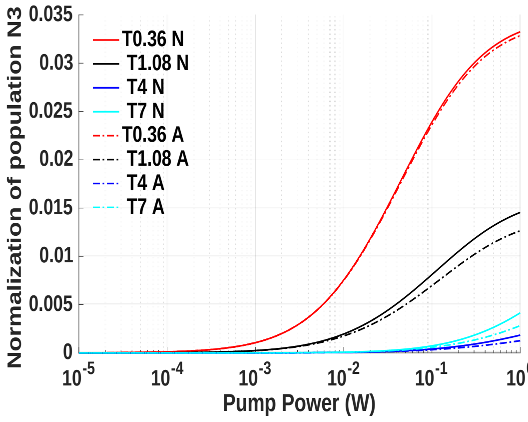

(c)

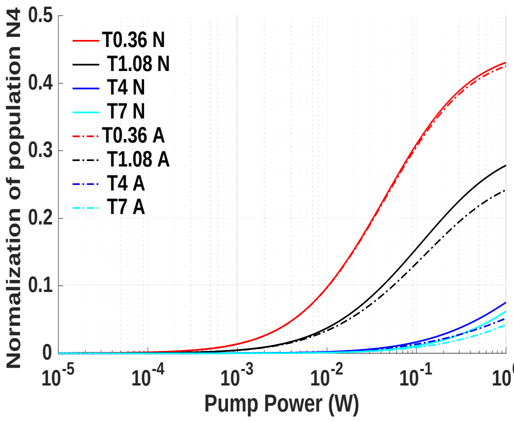

(d)

Fig. 8: The population of N_1,N_2,N_3 and N_4 levels for sample T0.36,T1.08,T4 and T7 using both numerical (N) and analytical (A) (solid lines numerical simulation) and (dot lines analytical simulation)

6. CONCLUSION

This paper shows the impact of the reverse cross relaxation on the various samples of Tm-deoped tellurite glass. This study has been able to define a set of spectroscopic parameters for Tm-doped tellurite glasses able to predict the reverse process over a wide doping level interval. To achieve this, it completed the available parameter with the inverse cross-relaxation process constant in Ref [13]. This paper proposed a method to assess the impact of the reverse cross-relaxation process. This method calculates the difference in calculations that occurs when neglecting reverse cross relaxation process and it assessed this difference over a range of doping levels. This method proved the validity of the approach used in the numerical simulation which used in the Reference [13] with respect the reverse cross relaxation. This paper also demonstrated that should be take into account the whole parameters including the reverse cross-relaxation process to performance simulations precisely. Within the aim of this paper, it showed that the appropriate calculation of reverse cross-relaxation parameter may have a significant effect on the simulation of laser and amplifier devices.

This set will allow laser engineering to appropriately simulate active device and to find the optimum doping level. This study also will enable scientists' laser to determine the appropriate glass for the desired application. It also will enable researchers to study and predict the behavior of thulium laser accurately, where this study take into account the whole set of parameters, including reverse cross-relaxation process.

7. ACKNOWLEDGMENTS

Wedad Albalawi acknowledges support of Cultural Bureau in London (UKSACB). This article is based upon work supported by Princess Nourah bint Abdulrahman University (PNU).

8. REFERENCES

[1] Hanna, D., Jauncey, I., Percival, R., Perry, I., & Smart, R. (1988). Continuous-wave oscillation of a monomode thulium-doped fibre laser. *Electronics Letters, 24*, 1222.

[2] Jackson, S. D., & Lauto, A. (2002). Diode- pumped fiber lasers: A new clinical tool. *Lasers in surgery and Medicine, 30*(3), 184-190.

[3] Allain, J., Monerie, M., & Poignant, H. (1989). Tunable CW lasing around 0.82, 1.48, 1.88 and 2.35 μmin thulium-doped fluorozirconate fibre. *Electronics Letters, 25*(24), 1660-1662.

[4] Scholle, K., Lamrini, S., Koopmann, P., & Fuhrberg, P. (2010). 2 μm laser sources and their possible applications *Frontiers in Guided Wave Optics and Optoelectronics*: InTech.

[5] Dobler, J. T., Braun, M., Nagel, J., Temyanko, V. L., Zaccheo, T. S., Harrison, F. W., . . . Kooi, S. A. (2013). *Applications of fiber lasers for remote sensing of atmospheric greenhouse gases.* Paper presented at the Proc. SPIE.

[6] Godard, A. (2007). Infrared (2–12 μm) solid-state laser sources: a review. *Comptes Rendus Physique, 8*(10), 1100-1128.

[7] Jackson, S. D., & King, T. A. (1999). Theoretical modeling of Tm-doped silica fiber lasers. *Journal of lightwave technology, 17*(5), 948.

[8] Evans, C. A., Ikonic, Z., Richards, B., Harrison, P., & Jha, A. (2009). Theoretical Modeling of a~2 μm Tm^{3+}Doped Tellurite Fiber Laser: The Influence of Cross Relaxation. *Lightwave Technology, Journal of, 27*(18), 4026-4032.

[9] Taher, M., Gebavi, H., Taccheo, S., Milanese, D., & Balda, R. (2011). Novel approach towards cross-relaxation energy transfer calculation applied on highly thulium doped tellurite glasses. *Optics Express, 19*(27), 26269-26274.

[10] Cornacchia, F., Sani, E., Toncelli, A., Tonelli, M., Marano, M., Taccheo, S., . . . Laporta, P. (2002). Optical spectroscopy and diode-pumped laser characteristics of codoped Tm-Ho: YLF and Tm-Ho: BaYF: a comparative analysis. *Applied Physics B: Lasers and Optics, 75*(8), 817-822.

[11] Simpson, D. A., Baxter, G. W., Collins, S. F., Gibbs, W., Blanc, W., Dussardier, B., & Monnom, G. (2006). Energy transfer up-conversion in Tm^{3+}-doped silica fiber. *Journal of non-crystalline solids, 352*(2), 136-141.

[12] Gebavi, H., Milanese, D., Balda, R., Chaussedent, S., Ferrari, M., Fernandez, J., & Ferraris, M. (2010). Spectroscopy and optical characterization of thulium

doped TZN glasses. *Journal of Physics D: Applied Physics, 43*(13), 135104.

[13] Albalawi, A., Varas, S., Chiasera, A., Gebavi, H., Albalawi, W., Blanc, W., . . . Taccheo, S. (2017). Determination of reverse cross-relaxation process constant in Tm-doped glass by $^3H_4$ fluorescence decay tail fitting. *Optical Materials Express, 7*(10), 3760-3768.

[14] Albalawi, A., Varas, S., Chiasera, A., Gebavi, H., Balda, R., Ferrari, M., & Taccheo, s. (2017). *Numerical investigation of reverse cross-relaxation process in Tm-doped glass by fitting $^3H_4$ fluorescence decay tail*. Paper presented at the Advanced Solid State Lasers (ASSL),, Nagoya, Japan.

[15] Kushida, T. (1973). Energy transfer and cooperative optical transitions in rare-earth doped inorganic materials. I. Transition probability calculation. *Journal of the physical society of Japan, 34*(5), 1318-1326.

[16] Walsh, B. M., Barnes, N. P., Petros, M., Yu, J., & Singh, U. N. (2004). Spectroscopy and modeling of solid state lanthanide lasers: Application to trivalent Tm^{3+} and Ho^{3+} in $YLiF_4$ and $LuLiF_4$. *Journal of Applied Physics, 95*(7), 3255-3271.

[17] McCumber, D. (1964). Einstein relations connecting broadband emission and absorption spectra. *Physical Review, 136*(4A), A954-A957.

[18] Gebavi, H., Milanese, D., Balda, R., Taccheo, S., Fernandez, J., Lousteau, J., & Ferraris, M. (2012). Spectroscopy of thulium and holmium heavily doped tellurite glasses. *Journal of luminescence, 132*(2), 270-276.